

A poly(urethane)-encapsulated benzo[2,3-*d*:6,7-*d'*]diimidazole organic down-converter for green hybrid LEDs

Alan A. Wiles^{a,‡}, Jochen Bruckbauer^{b,‡}, Nabeel Mohammed^{a,e,‡}, Michele Cariello^a, Joseph Cameron^a, Neil J. Findlay^a, Elaine Taylor-Shaw^b, David J. Wallis^{c,d}, Robert W. Martin^b, Peter J. Skabara^{a*} and Graeme Cooke^{a*}

^a WestCHEM, School of Chemistry, University of Glasgow, Glasgow, G12 8QQ, UK

^b Department of Physics, SUPA, University of Strathclyde, Glasgow, G4 0NG, UK

^c Department of Materials and Metallurgy, University of Cambridge, Cambridge, CB3 0FS, UK

^d Centre for High Frequency Engineering, University of Cardiff, Cardiff, CF24 3AA, UK

^e Department of Chemistry, College of Science, Kirkuk University, Kirkuk, Iraq

‡ These authors contributed equally to this work

Abstract

The development of organic down-converting materials continues to attract attention in hybrid LED technology by obviating the need for non-sustainable rare-earth elements. In this work, a benzodiimidazole-based system (**TPA-BDI**) has been employed as a down-converting layer in a hybrid organic-inorganic LED device. A commercially available poly(urethane)-based resin is used as the encapsulating material, providing a dilute layer of **TPA-BDI** that is deposited on top of the GaN-based LED. Crucially, the solution-state emissive performance is generally maintained when encapsulated at dilute concentrations within this resin. A maximum luminous efficacy of 87 lm/W was demonstrated using a 1.0 mg/ml concentration of **TPA-BDI** in the resin. The suitability of using organic down-converters to produce green light from hybrid devices was demonstrated by the excellent repeatability of the device characteristics across a series of encapsulated LEDs.

Introduction

Utilising organic emissive materials in display and lighting technologies has rapidly increased over the first part of the 21st century as light-emitting technologies have been developed to compete with user demand for efficient, high-performing devices (e.g. high-end mobile phone displays). Inorganic light-emitting diodes (LEDs) are ubiquitous in modern life, finding diverse applications ranging from displays through to automotive lighting.¹ Similarly, organic light-emitting diodes (OLEDs) are becoming increasingly common, particularly in display technologies as they can offer the consumer advantages including: highly efficient power conversion, excellent coverage of the colour spectrum, potential for use on flexible substrates/screens and a wide viewing angle.² Whilst both OLEDs and inorganic LEDs have become commonplace, hybrid inorganic/organic LEDs offer an alternative platform that combines the benefits of both material families.³⁻⁵ For example, hybrid devices offer an alternative approach to producing white light by replacing the inorganic phosphor component with a yellow-emissive organic material on top of a blue inorganic LED. This removes the requirement for traditional materials, for example cerium-doped yttrium aluminium garnet, and lessens the need for rare-earth materials in the face of ever-increasing consumer demand.⁶ This approach therefore combines high-performing electronic properties of inorganic blue LEDs with the broad and tuneable emission from organic semiconductors.⁷⁻⁹ We have previously reported molecular organic species as down-converter layers in hybrid LED devices, in combination with near-ultraviolet (near-UV) InGaN

LEDs,¹⁰ or more importantly, white light from combining blue-emitting GaN-on-Si LEDs with organic materials emitting yellow light.¹¹ This approach employed an electron-deficient tetrafluorobenzene core featuring fluorene-BODIPY arms and was designed to absorb light in the blue spectral range whilst emitting yellow light, affording overall white emission. More recently, a hybrid device with improved luminous efficacy and colour rendering was achieved through the use of a benzothiadiazole-based material as the down-converting layer.¹² We have also shown the potential for metal-organic frameworks (MOFs) to be used as the down-conversion layer when embedded within a suitable encapsulating material.¹³ Such a strategy rigidifies the down-converting material counteracting aggregation and luminescence quenching.

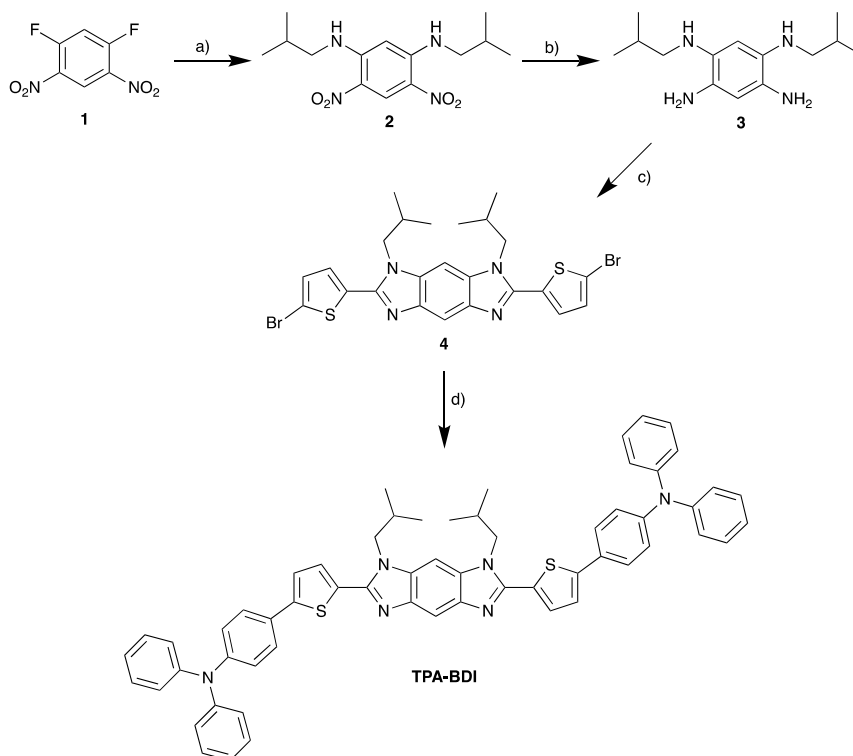
These examples predominantly highlight the effectiveness of hybrid approaches to achieving desirable white light emission. In LEDs, device performance is compromised if there is a lack of green light output, which is the wavelength region of the visible spectrum for which the human eye is most sensitive, resulting in a lower than desired luminous efficacy and unsatisfactory output for the consumer. Therefore, efficient green light sources are highly desirable to optimise overall device performance and consumer experience. Arguably the most common method of producing green light-emitting OLEDs is through the use of phosphorescent heavy metal atom-containing complexes as dopants within a guest matrix. The metal induces a strong spin-orbit coupling effect and enhances the emission efficiency by allowing emission from the triplet state, but these complexes require expensive and rare metals such as iridium.¹⁴ Alternatively, inorganic green LEDs can be fabricated using two semiconductor material systems, namely III-phosphides and III-nitrides. However, compared with their blue and red counterparts, the device efficiency of inorganic LEDs in the green spectral region is greatly reduced. This problem is referred to as the 'green gap' and much effort has been focussed towards advancing III-nitride LEDs in order to realise efficient green inorganic LEDs.¹⁵ An alternative approach is built on the commonly-used method employed for generating white LEDs, where a highly-efficient blue GaN-based inorganic LED is combined with a yellow emitting phosphor.

Herein, we discuss our efforts towards realising a molecular approach to enable green light emission from hybrid organic/inorganic materials by employing an efficient GaN-based inorganic LED with a layer of green-emitting organic material encapsulated within a commercially available optically transparent poly(urethane) resin. Optically transparent poly(urethane) resins are ubiquitous to LED applications, due to their excellent optical and mechanical properties and have largely been used as encapsulants. They also benefit from well-established, large scale, manufacturing techniques. Small molecules with a precise structure can offer advantages over polymeric semiconductor analogues, which can suffer from batch-to-batch variability and difficulties in achieving high purity.¹⁶ These advantages include complete reproducibility of synthesis and fine-tuning of properties for custom compatibility towards specific applications.¹⁷⁻¹⁹ We have synthesised the molecular species **TPA-BDI**, which is a novel benzodiimidazole-cored organic system that can be prepared in just four steps from commercially available starting materials. Benzodiimidazoles and their derivatives have previously been reported as having tuneable optical properties by using push-pull donor-acceptor components and the potential to have medium to high photoluminescence quantum yields.²⁰⁻²³ The application of **TPA-BDI** in down-converting hybrid LED devices is investigated by its incorporation into an optically transparent poly(urethane) resin as host and encapsulant.

Results and discussion

Synthesis

TPA-BDI was synthesised in four steps from 1,5-difluoro-2,4-dinitrobenzene **1** (scheme 1). An S_NAr reaction of **1** with isobutylamine gave compound **2** in high yield (90%). Subsequent reduction of the nitro moieties and condensation with 5-bromo-2-thiophenecarboxaldehyde afforded the key intermediate compound **4** in 47% yield over two steps. The final material **TPA-BDI** was obtained through Suzuki-Miyaura cross-coupling of **4** with 4-(diphenylamino)phenylboronic acid pinacol ester in moderate yield (59%). Full experimental details are available in the supporting information.



Scheme 1: synthesis of **TPA-BDI**; a) isobutylamine, K_2CO_3 , EtOH, reflux, 24h, 90%; b) $LiAlH_4$, THF, reflux, 16h; c) 5-bromo-2-thiophenecarboxaldehyde, glacial acetic acid, toluene, 80 °C, 72h, 47% over two steps; d) 4-(diphenylamino)phenylboronic acid pinacol ester, K_2CO_3 , $Pd(dba)_2$, 1,4-dioxane, 90 °C, 24h, 55%.

Optical properties

We tested the compatibility of the dye with a commercial poly(urethane) resin (Opti-tectm 4200). This material is a two-part resin (resin to hardener ratio 1:1) and is marketed to have very good UV stability and high transparency. **TPA-BDI** was first dissolved in part A of the resin and sonicated for 1 minute until homogeneous dispersion was observed. An equal amount of the hardener (Part B) was then added and the composite was mixed and further sonicated for 30 seconds. After drop-casting, the mixture was then cured at 40°C for 24 hours. Initial observations showed that **TPA-BDI** disperses homogeneously through both part A and part B of the resin and gives a homogeneous dispersion in the hardened films up to a ratio of 20 mg/ml (concentration in volume of combined part A and part B).

The absorbance and fluorescence of **TPA-BDI** were analysed in the solution state (Figure 1a) and in the hardened resin (Figure 1b). In dichloromethane solutions, **TPA-BDI** shows an absorption maximum at 422 nm ($\epsilon = 132,810 \text{ L mol}^{-1} \text{ cm}^{-1}$) and an emission maximum at 479 nm and a shoulder at 506 nm (Figure 1a).

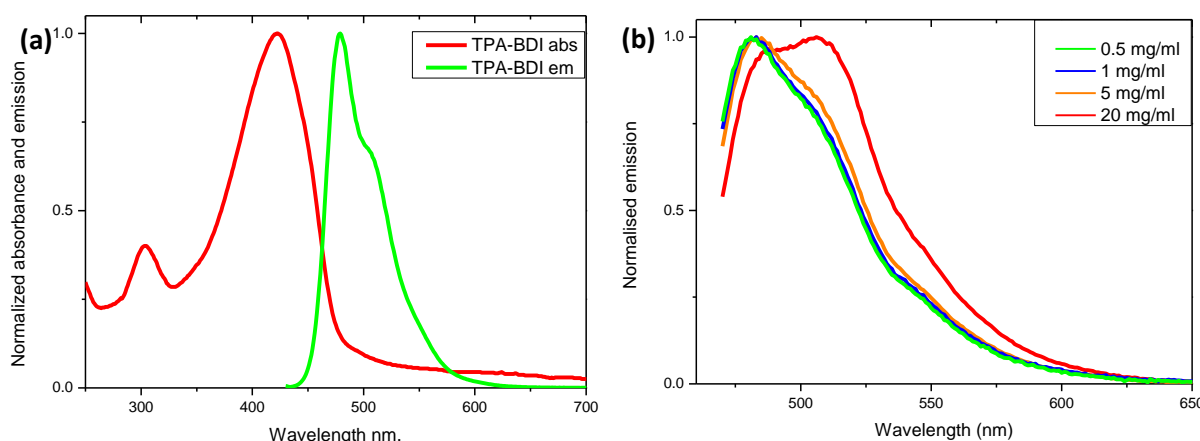


Figure 1: a) solution-state absorbance and emission spectra of **TPA-BDI** (1×10^{-5} M in dichloromethane, excitation wavelength 426 nm); b) normalised emission spectra (excitation at 426 nm) of **TPA-BDI** as a hardened film with concentrations of 0.5 mg/ml (green line), 1 mg/ml (blue line), 5 mg/ml (orange line) and 20 mg/ml (green line).

Absorption spectra of the hardened films are essentially identical with only a very small red-shift in the absorbance maximum to 426 nm (vs 422 nm in solution), and only the addition of a band at 344 nm which can be attributed to the resin (Figure S1a). Higher concentrations showed a small red-shift in the onset of absorbance (480 nm to 500 nm), consistent with aggregation effects. However, the spectra were highly saturated in concentrations above 0.5 mg/ml due to instrument limitations (Figure S1a). Fluorescence spectroscopy of **TPA-BDI** was carried out at varying concentrations of the encapsulated hardened films (Figure 1b). For clarity, only emission at 0.5 mg/ml, 1 mg/ml, 5 mg/ml and 20 mg/ml are shown. We can see that the emission spectrum of **TPA-BDI** is only slightly red-shifted at low concentrations when compared with the solution-state spectrum with a maximum at 484 nm (vs 479 nm in solution), again consistent with small aggregation effect in the hardened resin. The spectral shape of the emission spectra is essentially retained at low concentrations (up to 5 mg/ml). However, with increasing concentration, the emission is broadened and red-shifted and the spectral shape changes in line with increasing levels of aggregation with a significant increase in contribution from the low-energy shoulder peak at 506 nm. Additionally, the photoluminescence quantum yield (PLQY) of **TPA-BDI** in dichloromethane (1×10^{-4} M) was found to be 55% , and 49% and 44% in the hardened resin (1 mg/ml and 5 mg/ml, respectively). Overall, the emission characteristics of **TPA-BDI** at low concentrations in the resin (0.5 mg/ml up to 5 mg/ml), are similar to the solution-state measurements. An increase in concentration of **TPA-BDI** in the resin clearly leads to aggregation-induced quenching of emission.

Down-converting devices

The InGaN/GaN LEDs chosen for this work emit at a wavelength of about 450 nm and are based on Plessey's "GaN-on-Silicon" technology. **TPA-BDI** was dissolved in a commercial poly(urethane) resin (Opti-tec™ 4200) containing a hardener (1:1 ratio), at different concentrations of 0.5, 1.0, 2.5 and 5.0 mg/ml and deposited on top of the blue LED chip to form a homogeneous film with high transparency (Figure S2).

Figure 2(a) shows the absolute, response-corrected electroluminescence (EL) spectra of the LEDs with different concentrations of **TPA-BDI** operated under a constant forward current of 25 mA. As a reference the spectrum of the bare blue LED without the converter is also shown. While the blue peak associated with transmitted, not absorbed, light from the blue LED is dominant for the lowest

concentration of 0.5 mg/ml, more of the light is absorbed and re-emitted in the green spectral range of 480-600 nm for the higher concentrations. The green emission maximum is around 510 nm. Even at 1 mg/ml almost all the light from the blue LED is absorbed by the organic molecule. The intensity of the green emission peak decreases with increasing concentration and also exhibits a slight change in spectral shape. Both can be attributed to quenching of the luminescence due to increased aggregation at higher concentrations.

The chromaticity coordinates in the CIE 1931 diagram for the LEDs featuring different concentrations of **TPA-BDI** are displayed in Figure 2(b). Increasing the concentration shifts the chromaticity coordinates steadily from the blue region (bottom left corner) towards the green region. The obvious deviation from a straight line observed when using the highest concentration (5.0 mg/ml) is due to the change in spectral shape of the emission of the hybrid device. This addition of red in the emission spectrum shifts the chromaticity coordinate to the right (pure red is located in the right corner in the diagram).

To quantify the conversion process, the luminous efficacy and the radiant flux are determined from the absolute EL spectra. The luminous efficacy is the ratio of the luminous flux and the electrical input power of the LED measured in lm/W. It describes the efficiency of converting electrical power into light taking the human eye response into account and is commonly used to describe white LEDs.^{13, 24} The radiant flux is the total optical power measured in W, whereas the luminous flux is the perceived optical power in lm (lumens) taking the eye response into account. The luminous efficacy values for the LED using different concentrations of **TPA-BDI** can be found in Table 1. The increase in luminous efficacy between the two LEDs with the lowest concentrations (0.5 and 1.0 mg/ml), relates to the increased contribution in the green spectral range despite the reduced blue emission. As the green emission peak decreases with increasing concentrations this concomitantly causes a drop in the luminous efficacy. Although the luminous efficacy is generally used to measure the performance of white LEDs, it is not the best measure for green LED performance. Therefore, the radiant flux is used for describing the efficiency of the colour conversion. Table 1 also shows the radiant flux of the blue LEDs before they were coated with the organic material as well as the radiant flux of the same LEDs measured after applying the colour converter. From these measurements, the loss in radiant flux is calculated as listed in Table 1. The radiant flux is decreasing with increasing concentration since the intensity of both emission peaks decreases with increasing concentration. This is also reflected by the radiant flux loss. The best result is achieved for the green LED with a 1.0 mg/ml concentration. At this concentration 51% of the optical power (radiant flux) from the blue LED is converted into green emission; this is equivalent to a radiant flux loss of 49%. With increasing concentration, the intensity drops further and above 5.0 mg/ml the spectral shape starts to change as the emission of the down-converter becomes red-shifted.

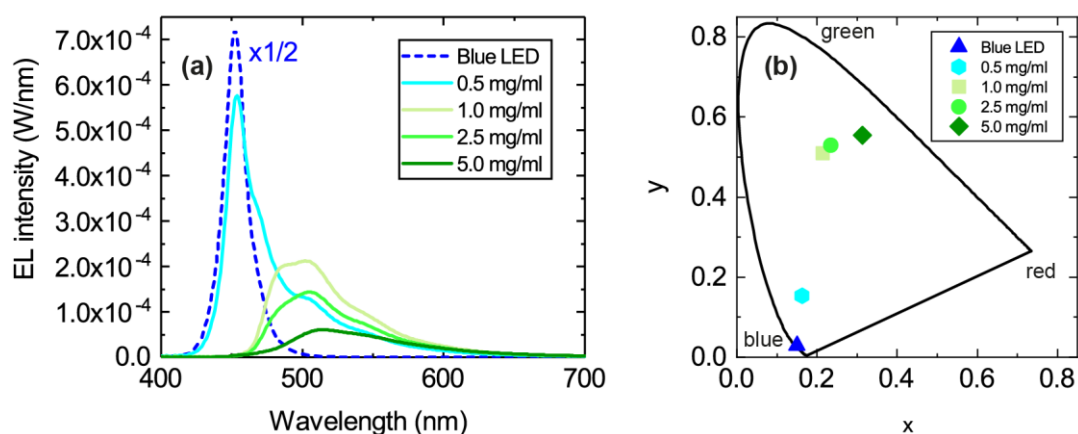


Figure 2: (a) Absolute EL spectra of the blue LEDs coated with the organic colour converter using concentrations of 0.5, 1.0, 2.5 and 5.0 mg/ml. The spectrum of the blue LED is scaled down by a factor of 2. (b) CIE 1931 chromaticity coordinates of the same LEDs.

Table 1: Luminous efficacy, radiant flux before and after deposition of the organic material and loss in radiant flux of the hybrid LEDs of the concentration series.

Concentration (mg/ml)	Luminous efficacy (lm/W)	Radiant flux (mW) – hybrid LED (after)	Radiant flux (mW) – blue LED (before)	Radiant flux loss (%)
0.5	60	25	33	24
1.0	87	17	33	49
2.5	64	12	31	63
5.0	39	6	33	81

This loss in intensity of the hybrid LED devices can be explained by several photophysical factors. First, reabsorption of the emitted photons could have some effect due to the small overlap of the absorption and emission peak of **TPA-BDI**. As previously mentioned, aggregation-induced quenching effects are also responsible for some of the loss in intensity particularly when increasing the concentration. Secondly, photo-induced absorption (PIA) is likely the largest contributor to this loss in intensity, as explained in a previous publication.¹³ The effect of PIA was tested by means of pulsing the applied current (2% duty cycle, 500 μ s period) to the blue LED encapsulated with a 1 mg/ml of **TPA-BDI** in the resin. Compared with the continuous current measurement of the same device, the intensity of the emission peak is higher by a factor of about 1.5 as seen in Figure 3. The radiant flux loss for this pulsed device is 38% compared with 60% when continuously driven. Here, the pulse regime allows for any triplet states to relax within the timescale of the pulse (500 μ s) thereby inhibiting the constant population of triplet states which will affect the ability of the organic molecule to emit while under constant illumination. In other words, by pulsing the blue LED, less of the blue light is wasted in non-radiative processes, leading to an increase in radiant flux.

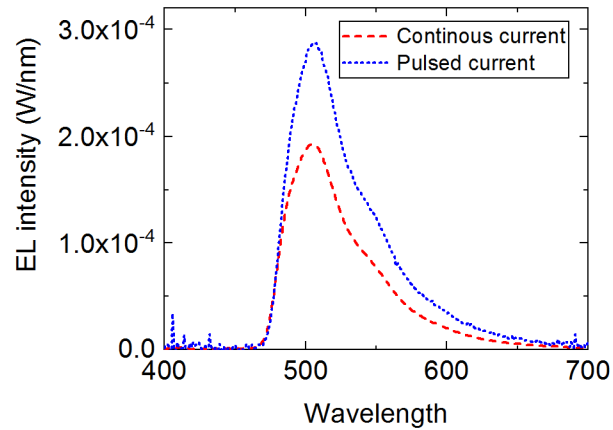


Figure 3: EL spectrum of the same hybrid LED operated with a continuous or pulsed current of 25 mA.

Lifetime and degradation

The degradation of the 1.0 mg/ml hybrid LEDs was studied by continuously driving the LEDs for about 3000 minutes under a constant forward current of 25 mA and recording an EL spectrum at different time intervals. The EL spectra are shown in Figure 4(a). The green emission peak decreases, whereas the blue emission peak increases with time. This redistribution of the two emission peaks also causes the chromaticity coordinates to move towards the blue corner since the blue LED peak becomes more dominant over time as seen in Figure S4(b). Similarly, the radiant flux initially drops with decreasing green emission and then increases once the emission from the blue LED becomes dominant again (Figure 4(b)). In contrast, the luminous flux only decreases because of the reduced green emission, since the human eye is more sensitive in that spectral range (Fig. S4(d)).

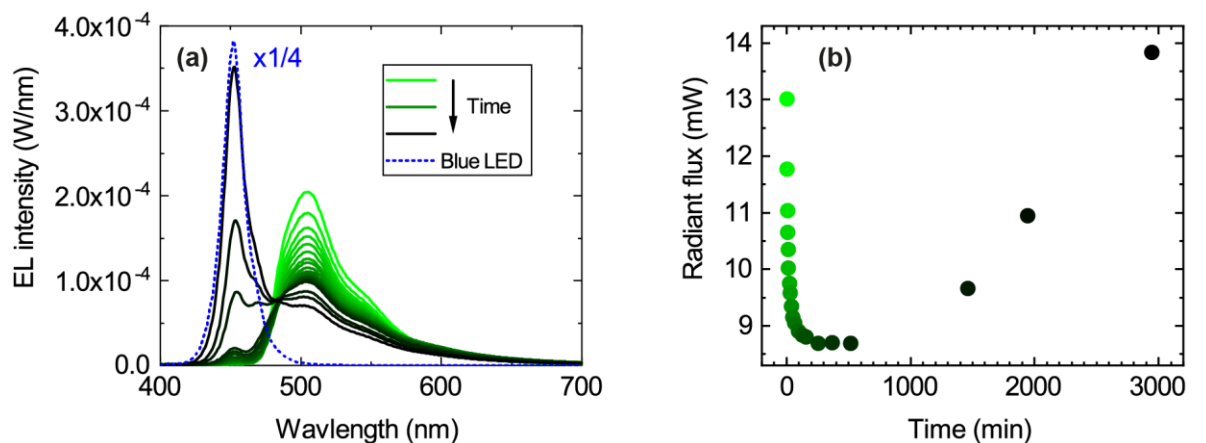


Figure 4: A hybrid green LED with 1.0 mg/ml of the colour converter was continuously driven using 25 mA for 3000 minutes. (a) EL spectra were recorded at different time intervals and (b) the radiant flux plotted as a function of operating time.

Degradation of the transparent encapsulant can be excluded since a similar measurement series was performed using the resin without the organic colour converter (see Figure S5), and showed no degradation of the encapsulant. Therefore, this points towards the degradation of the organic material encapsulated in the resin. Thermal degradation of the organic material is unlikely as it is thermally stable up to 477 °C and its glass transition temperature (T_g) is 262 °C (measured by

thermogravimetric analysis (TGA) and differential scanning calorimetry (DSC), Figure S3), both temperatures are well above the operating temperature of the blue LED.

The same LEDs were measured again after approximately 21 months in order to observe any change over time when the LEDs were not operated. Figure S6a shows the last EL spectrum of the hybrid LED (1 mg/ml) that had been subjected to 3000 minutes of constant irradiation and the same device after 21 months. Figure S6b, on the other hand, shows the initial EL spectrum of another device (1 mg/ml concentration) that had been operated only once for no more than 10 min, and then compared with the EL spectrum measured after 21 months using a continuous or pulsed current. As can be seen, the emission spectrum of both devices does not change over time. This means that the initial degradation of the organic material is limited and that the material is efficiently protected by the encapsulant from the environment to avoid further degradation by oxygen and moisture. Therefore, degradation of the organic material is likely due to a more complex photodegradation process which will require further studies.

Reproducibility

To investigate the reproducibility of the devices, four nominally identical hybrid LEDs were prepared using a concentration of 1.0 mg/ml. The EL spectra are shown in Figure S7(a). The spectra of LEDs #1-3 are almost identical, whereas the EL spectrum for LED #4 is slightly more intense, but the spectral shape is the same. This is most likely caused by a slightly different volume of the colour converter deposited on this LED during drop-casting. This trend is also evidenced in the luminous efficacy and the radiant flux loss (Table S8). LED #4 had possibly a larger volume of the colour converter deposited since the luminous efficacy is higher and the radiant flux loss smaller, implying that there is more green emission. LED #4 is more comparable to the equivalent 1.0 mg/ml hybrid LED of the concentration series in Figure 1 and Table 1. The chromaticity coordinates (Figure S7(b)) are similar for all four LEDs, because the spectral shape of the emission spectra are comparable. Overall, the results are consistent, especially when the volume of the deposited colour converter is carefully controlled.

Summary

We have reported the synthesis, characterisation and hybrid device performance of a benzodiimidazole-based small-molecule down-converter (**TPA-BDI**). The molecule exhibits almost identical optical properties when dispersed within a commercially available optically transparent poly(urethane) resin. The resin can be deposited onto inorganic GaN-based LEDs and cured to encapsulate the LED and form a down-conversion layer. It has been shown that these hybrid devices provide green light emission using a low concentration of **TPA-BDI** (1 mg/ml) within the encapsulating resin. We have also shown that operating the hybrid device under pulsed conditions leads to a 1.5x increase in the intensity of the device and a minimised radiant flux loss of 38% compared to 60% under constant illumination by suppressing non-radiative processes from triplet states. Although some evidence of decomposition is observed across the timeframe studied, high reproducibility in the emissive performance was recorded across a series of LEDs that were encapsulated. This highlights the potential of using an optically transparent poly(urethane) host and encapsulant for organic down-converters in hybrid devices.

Acknowledgements

NM thanks the Ministry of Higher Education and Scientific Research of Iraq and the University of Kirkuk. DJW would like to acknowledge financial support from EPSRC through a Manufacturing Fellowship (EP/N01202X/2). JC and NJF also thank the EPSRC for funding (EP/P02744X and EP/R03480X).

References

1. M. Bessho and K. Shimizu, *Electr. Commun. Jpn*, 2012, **95**, 1-7.
2. Y. R. Cho, H. S. Kim, Y.-J. Yu and M. C. Suh, *Sci. Rep.*, 2015, **5**, 15903.
3. P. Schlotter, R. Schmidt and J. Schneider, *J. Appl. Phys. A*, 1997, **64**, 417-418.
4. F. Hide, P. Kozodoy, S. P. DenBaars and A. J. Heeger, *Appl. Phys. Lett.*, 1997, **70**, 2664-2666.
5. Z. Yue, Y. F. Cheung, H. W. Choi, Z. Zhao, B. Z. Tang and K. S. Wong, *Opt. Mater. Express*, 2013, **3**, 1906-1911.
6. C. Zhang and A. J. Heeger, *J. Appl. Phys.*, 1998, **84**, 1579-1582.
7. G. Heliotis, P. N. Stavrinou, D. D. C. Bradley, E. Gu, C. Griffin, C. W. Jeon and M. D. Dawson, *Appl. Phys. Lett.*, 2005, **87**, 103505.
8. E. Gu, H. X. Zhang, H. D. Sun, M. D. Dawson, A. R. Mackintosh, A. J. C. Kuehne, R. A. Pethrick, C. Belton and D. D. C. Bradley, *Appl. Phys. Lett.*, 2007, **90**, 031116.
9. V. M. Agranovich, Y. N. Gartstein and M. Litinskaya, *Chem. Rev.*, 2011, **111**, 5179-5214.
10. N. J. Findlay, C. Orofino-Peña, J. Bruckbauer, S. E. T. Elmasly, S. Arumugam, A. R. Inigo, A. L. Kanibolotsky, R. W. Martin and P. J. Skabara, *J. Mater. Chem. C*, 2013, **1**, 2249-2256.
11. N. J. Findlay, J. Bruckbauer, A. R. Inigo, B. Breig, S. Arumugam, D. J. Wallis, R. W. Martin and P. J. Skabara, *Adv Mater*, 2014, **26**, 7290-7294.
12. J. Bruckbauer, C. Brasser, N. J. Findlay, P. R. Edwards, D. J. Wallis, P. J. Skabara and R. W. Martin, *J. Phys. D: Appl. Phys.*, 2016, **49**, 405103.
13. E. Taylor-Shaw, E. Angioni, N. J. Findlay, B. Breig, A. R. Inigo, J. Bruckbauer, D. J. Wallis, P. J. Skabara and R. W. Martin, *J. Mater. Chem. C*, 2016, **4**, 11499-11507.
14. E. Angioni, R. J. Marshall, N. J. Findlay, J. Bruckbauer, B. Breig, D. J. Wallis, R. W. Martin, R. S. Forgan and P. J. Skabara, *J. Mater. Chem. C*, 2019, **7**, 2394-2400.
15. H. Xu, R. Chen, Q. Sun, W. Lai, Q. Su, W. Huang and X. Liu, *Chem. Soc. Rev.*, 2014, **43**, 3259-3302.
16. M. Auf der Maur, A. Pecchia, G. Penazzi, W. Rodrigues and A. Di Carlo, *Phys. Rev. Lett.*, 2016, **116**, 027401.
17. M. Zhu and C. Yang, *Chem. Soc. Rev.*, 2013, **42**, 4963-4976.
18. A. L. Kanibolotsky, I. F. Perepichka and P. J. Skabara, *Chem. Soc. Rev.*, 2010, **39**, 2695-2728.
19. A. L. Kanibolotsky, N. Laurand, M. D. Dawson, G. A. Turnbull, I. D. W. Samuel and P. J. Skabara, *Acc. Chem. Res.*, 2019, **52**, 1665-1674.
20. J. Schönamsgruber and A. Hirsch, *Eur. J. Org. Chem.*, 2015, **2015**, 2167-2174.
21. M. Tasiar, V. Hugues, M. Blanchard-Desce and D. T. Gryko, *Chem. Asian J.*, 2012, **7**, 2656-2661.
22. H.-F. Chen, Y.-M. Cui, J.-G. Guo and H.-X. Lin, *Dyes Pigments*, 2012, **94**, 583-591.
23. X.-J. Lin, Z. Shen, H.-J. Xu, Y.-Z. Li, H.-T. Zhang and X.-Z. You, *Inorg. Chem. Commun.*, 2004, **7**, 1167-1169.
24. E. Taylor, P. R. Edwards and R. W. Martin, *Phys. Status Solidi A*, 2012, **209**, 461-464.